Optimal control strategies-based maximum power point tracking for photovoltaic systems under variable environmental conditions

Sally Abdulaziz, Galal Atlam, Gomaa Zaki, Essam Nabil

Optimal control strategies-based maximum power point tracking for photovoltaic systems under variable environmental conditions

Sally Abdulaziz*, Galal Atlam, Gomaa Zaki and Essam Nabil

Department of Industrial Electronics and Control Engineering,
Faculty of Electronic Engineering,
Menoufia University, Egypt
Email: sally.abdulaziz@yahoo.com
Email: galal.atlam@el-eng.menofia.edu.eg
Email: gomaazaki54@yahoo.com
Email: essam.abdelaziz@el-eng.menofia.edu.eg
*Corresponding author

Abstract: To increase the efficiency of photovoltaic (PV) array output under variable environmental conditions, maximum power point tracking (MPPT) of the solar arrays is needed. This paper proposes fuzzy logic controller (FLC)-based MPPT, artificial neural network (ANN)-based MPPT, neuro-fuzzy (NF)-based MPPT, particle swarm optimisation (PSO)-based MPPT, and cuckoo search (CS) algorithm-based MPPT to combine an adaptive controller and an optimisation, to guarantee global stability and a constant settling time for all operation conditions. This combination enables an increase in the power generated in comparison with conventional MPPT techniques. Simulation results show that the proposed photovoltaic/storage generator is able to supply the suggested dynamic loads under different conditions, and achieve good performance. It is also noticed that operating the photovoltaic array based on maximum power point tracking conditions gives about 43% extra power generation than in the case of normal operation.

Biographical notes: Sally Abdulaziz received her BSc degree in Electronic Engineering (Industrial Electronics and Control Engineering) in 2010, Department of Industrial Electronics and Control Engineering, Faculty of Electronic Engineering, Menoufia University. She is interested in electrical engineering work and works as an Electrical engineer in an industrial factory in Sadat City, Menoufia, Egypt.

Galal Atlam received his BSc in Electronic Engineering in Industrial Electronics and Control Engineering in 1977, MSc in Electronic Engineering in Automatic Control Engineering in 1988, and PhD in Electronic Engineering in Control Engineering and Systems in 1997 at the Department of Industrial Electronics and Control Engineering, Faculty of Electronic Engineering, Menoufia University. From 1977 to 1988, he was a demonstrator (Teaching Assistant) in the Industrial Electronics and Control Engineering Department, Faculty of Electronic Engineering, Menoufia University. From 1988 to 1997, he was an Assistant Lecturer in the Industrial Electronics and Control Engineering Department, Faculty of Electronic Engineering, Menoufia University. From 1997 to 2015, he was an Assistant Professor in the Industrial Electronics and Control Engineering Department, Faculty of Electronic Engineering, Menoufia University. Since 2015, he was a Professor Emeritus in the Industrial Electronics and Control Engineering department, Faculty of Electronic Engineering, Menoufia University.

Gomaa Zaki received his BSc in Electronic Engineering in Industrial Electronics and Control Engineering in 1976, MSc in Electronic Engineering in Automatic Control Engineering in 1982, and PhD in Electronic Engineering in Control Engineering and Systems in 1990 at the Department of Industrial Electronics and Control Engineering, Faculty of Electronic Engineering, Menoufia University. From 1976 to 1982, he was a demonstrator (Teaching Assistant) in the Industrial Electronics and Control Engineering Department, Faculty of Electronic Engineering,

Menoufia University. From 1982 to 1990, he was an Assistant Lecturer in the Industrial Electronics and Control Engineering Department, Faculty of Electronic Engineering, Menoufia University. From 1990 to 2014, he was an Assistant Professor in the Industrial Electronics and Control Engineering Department, Faculty of Electronic Engineering, Menoufia University. Since 2014, he was a Professor Emeritus in the Industrial Electronics and Control Engineering department, Faculty of Electronic Engineering, Menoufia University.

Essam Nabil received his BSc in Electronic Engineering in Industrial Electronics and Control Engineering in 2006, MSc in Electronic Engineering in Automatic Control Engineering in 2011, and PhD in Electronic Engineering in Control Engineering and Systems in 2016 at the Department of Industrial Electronics and Control Engineering, Faculty of Electronic Engineering, Menoufia University. From 2006 to 2011, he was a demonstrator (Teaching Assistant) in the Industrial Electronics and Control Engineering Department, Faculty of Electronic Engineering, Menoufia University, and Supervisor and Chairman of Organizing and Arbitration Committees of the permanent Scientific Exhibition of Industrial Electronics and Control Engineering Department, Faculty of Electronic Engineering, Menoufia University

1 Introduction

The energy crisis is the most critical issue threatening the world today because conventional energy sources, such as coal, oil and natural gas are finite. Also, carbon dioxide produced by burning fossil fuels causes climate change. Thus, the use of renewable energy sources, such as wind, solar, geothermal, and biomass resources, is an urgent requirement. The focus of this paper is on solar energy because its advantages surpass the advantages of other resources. Solar energy is clean, noiseless and renewable. It does not produce greenhouse gases, which cause environmental pollution or contamination. It can be generated at any place where sunlight is available and is useful in places where establishing an electricity grid is difficult (Abouadane et al., 2017). Electricity can be generated from solar energy, using either a direct method or an indirect method; the direct method uses photovoltaic systems and the indirect method uses optical devices, which provide steam to propel a turbine and generate electricity (Camacho et al., 2010). This paper discusses the direct method.

Photovoltaic systems are preferred in distributed generation (DG) because electricity generators can be located close to the loads (Gonzalez-Longatt, 2005). The most crucial advantage of DG is power saving, as during the transmission of power from the power source to the user, 4.2%–8.9% of the power can get wasted because the equipment used for power transmission is quite old (Ilyas et al., 2013).

Photovoltaic systems have two main disadvantages, namely their high installation cost and their low efficiency (Dolara et al., 2009). To reduce their cost of generating 1 kilowatt hour, the efficiency of photovoltaic systems has to be increased by using a dynamic tracking algorithm to track the maximum operating point, especially when the solar radiation and ambient temperature change. There are two types of maximum power point trackers: mechanical trackers and electronic trackers. Mechanical trackers direct the photovoltaic panel to track the sun using single or dual-axis trackers (Alexandru, 2019; Tudorache and Kreindler, 2010). Since these mechanical trackers have

disadvantages, such as complexity, low efficiency, and high cost, electronic trackers are always preferred.

Electronic maximum power point tracking (MPPT) techniques can be categorised into three classes: conventional, soft computing and optimisation-based MPPT techniques. Conventional MPPT techniques include the fractional open circuit voltage (FOCV) technique (Ahmad, 2010), the fractional short circuit current (FSCC) technique (Sher et al., 2015), the perturb and observe (P&O) technique (Sera et al., 2013), and the incremental conductance (INC) technique (Safari and Mekhilef, 2010). As adaptive controllers have proved their efficiency over classical control methods (Wang et al., 2020; Wang. 2021), soft computing algorithms are used in MPPT. These algorithms include fuzzy logic controllers (FLCs) (Chim et al., 2011; Rajavel and Prabha, 2020), artificial neural networks (ANNs) (Hiyama and Kitabayashi, 1997; Elobaid et al., 2012), and neuro-fuzzy (NF) controllers (Abido et al., 2015; Douiri, 2019), which are also used to track the maximum power points of photovoltaic systems. To further improve the efficiency of MPPT, optimisation-based MPPT techniques are used, including genetic algorithms (GAs) (Dahmane et al., 2013), differential evolutionary (DE) algorithms (Tajuddin et al., 2013), particle swarm optimisation (PSO) algorithms (Figueiredo et al., 2019), ant colony optimisation (ACO) algorithms (Titri et al., 2017), artificial bee colony (ABC) algorithms (Soufyane Benyoucef et al., 2015), grey wolf optimisation (GWO) algorithms (Mohanty et al., 2015) and cuckoo search (CS) algorithms (Ahmed and Salam, 2013).

Increasing the efficiency of MPPT has been the focus of many researchers in the last decade. As stated in Saidi et al. (2019), Feroz Mirza et al. (2020) and Baimel et al. (2019), considerable research has been done on modifying conventional methods to improve their efficiency. For this purpose, the use of hybrid algorithms, which combine two algorithms to increase the MPPT efficiency (Labeeb et al., 2016; Padmanaban et al., 2019), has been employed. The speed, cost, complexity, number of sensors used, and dynamic and steady-state efficiencies of the different MPPT techniques vary. Thus, power engineers have to carefully

consider the advantages of each technique in selecting the most effective technique for an application (Ezinwanne et al., 2017).

In this paper, the PSO algorithm with changing inertia weight is discussed, as many researchers have stated that the PSO with fixed inertia weight has a weakness in tracking the maximum power point. To highlight the proposed algorithm's efficiency in tracking the MPPT, it is compared to conventional methods, soft computing methods, and the CS algorithm under constant, gradually changing, and rapidly changing atmospheric conditions, in addition to partial shading conditions. The paper is organised as follows: Section 2 presents a sample photovoltaic system, Section 3 is the preliminary, Section 4 proposed optimal MPPT techniques, Section 5 presents the simulation results, and Section 6 presents the concluding remarks.

2   Photovoltaic system

A stand-alone photovoltaic system consists of a photovoltaic array, a charge controller, a battery bank, an inverter, and the loads (Figure 1). A photovoltaic array converts sunlight into electrical energy. The charge controller consists of a DC-DC converter and an MPPT algorithm. The MPPT algorithm controls the DC-DC converter duty cycle. This takes place in order to match the internal resistance of the photovoltaic array to the load's resistance and deliver maximum power. A DC-AC inverter converts the generated electricity from DC to AC to feed the AC loads. The battery bank is used to store any excess electricity, for use at night or during cloudy days.

2.1   Modelling of photovoltaic array

The single-diode model and the double-diode model are the two most commonly used photovoltaic models (Figure 2). The single-diode model is more popular and simpler than the double-diode model, although the latter provides more accurate results than the former (Eltamaly et al., 2019).

Figure 1   A stand-alone photovoltaic system (see online version for colours)
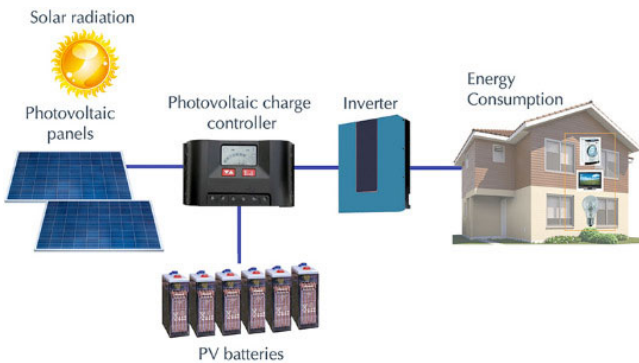
Figure 2   Photovoltaic cell models (a) single-diode model and (b) double-diode model

(a)

(b)
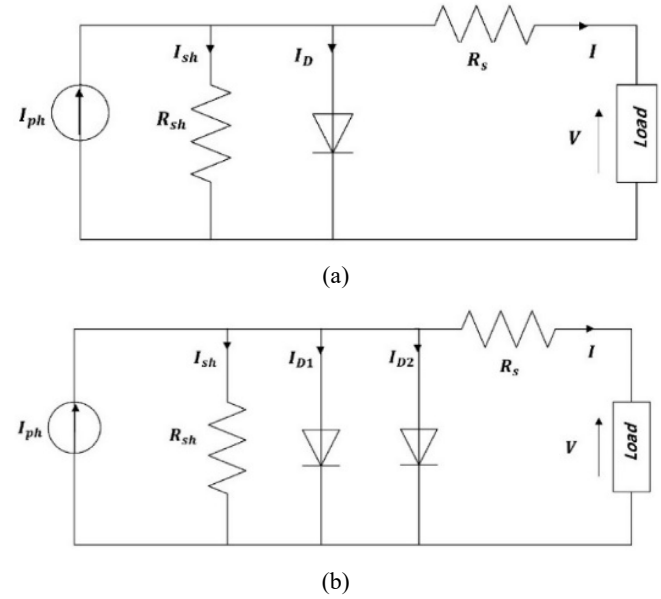
The single-diode photovoltaic model can be represented by a photocurrent source connected to a resistance in series and a diode and a shunt resistance in parallel. To simplify the model, the resistances can be neglected, although the model will then be less reliable. The single-diode model can be represented by equation (1):

$$I_{pv} = I_{ph} - I_s \left[\exp\left(\frac{V_{pv} + I_{pv}R_s}{I_f V_{th}} \right) - 1 \right] - \frac{V_{pv} + I_{pv}R_s}{R_{sh}} \qquad (1)$$

where I_{pv} and V_{pv} are the photovoltaic output current and voltage, respectively. I_{ph} is the photo generated current, I_s is the diode saturation current, I_f is the diode ideality factor, R_s and R_{sh} are the series and shunt resistances, respectively, and V_{th} is the thermal voltage defined in equation (2).

$$V_{th} = {K_B T_a} \big/ {q_c} \qquad (2)$$

where K_B is the Boltzmann's constant ($K_B = 1.38 \times 10^{-23}$ J/K), T_a is the ambient temperature, and q_c is the electron charge ($q_c = 1.6 \times 10^{-19}$ C).

The double-diode photovoltaic model is similar to the single-diode model, with one additional parallel diode. The following equation represents the double-diode model:

$$I_{pv} = I_{ph} - I_{s1} \left[\exp\left(\frac{V_{pv} + I_{pv}R_s}{I_f V_{th}} \right) - 1 \right]$$
$$- I_{s2} \left[\exp\left(\frac{V_{pv} + I_{pv}R_s}{I_f V_{th}} \right) - 1 \right] - \frac{V_{pv} + I_{pv}R_s}{R_{sh}} \qquad (3)$$

Figure 3 Photovoltaic array structures (a) series-parallel (SP) (b) bridge link and (c) total crossed tie structures (see online version for colours)

(a)

(b)

(c)
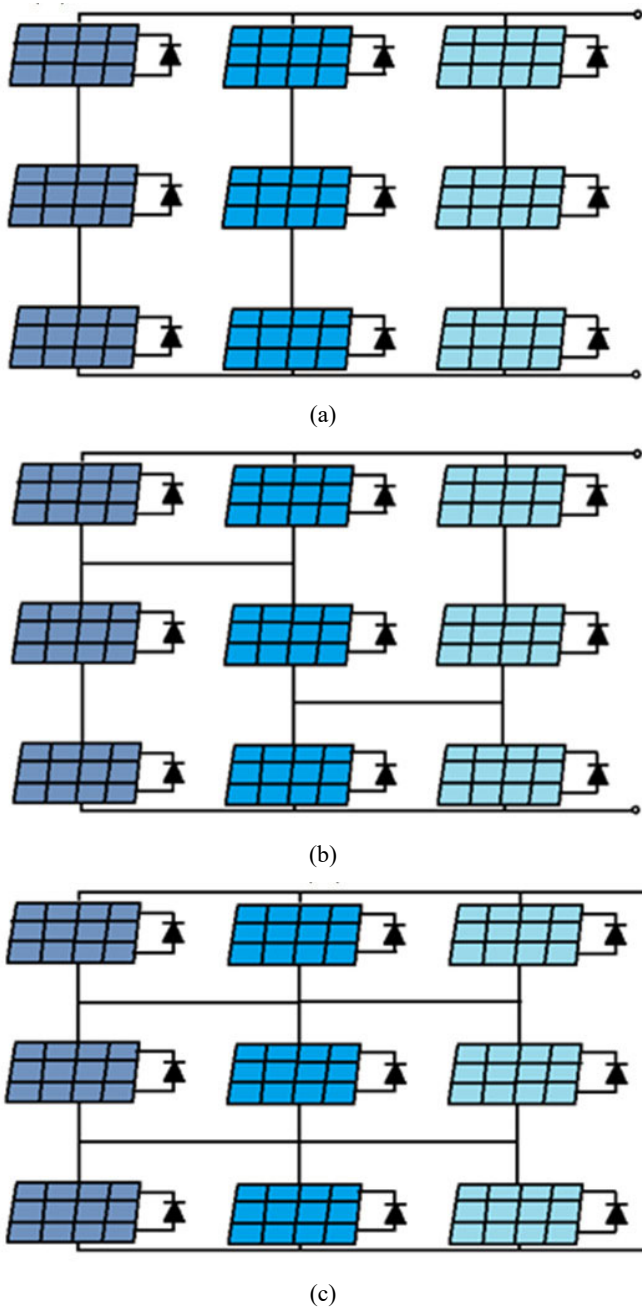
Since the amount of power generated by a PV cell is small, the cells can be connected in series or in parallel, to produce a higher voltage or a higher current, respectively. A photovoltaic module is obtained by connecting several photovoltaic cells. Many modules can be connected to construct a photovoltaic array, to produce the desired voltage and current. Three methods are available to connect photovoltaic arrays (Zou et al., 2020) (Figure 3).

Figures 4 and 5 show the characteristics of the photovoltaic current-voltage (I-V) and power-voltage (P-V), respectively, of a single-diode model-based photovoltaic system, under changing atmospheric conditions.

Figure 4 Photovoltaic I-V characteristics for (a) different solar irradiance levels and (b) different ambient temperature (see online version for colours)

(a)

(b)
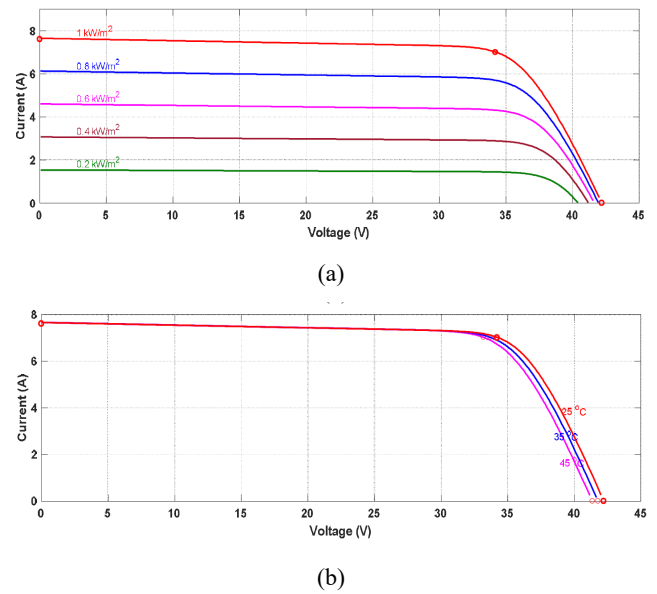
Figure 5 Photovoltaic P-V characteristics for (a) different solar irradiance levels and (b) different ambient temperature (see online version for colours)

(a)

(b)
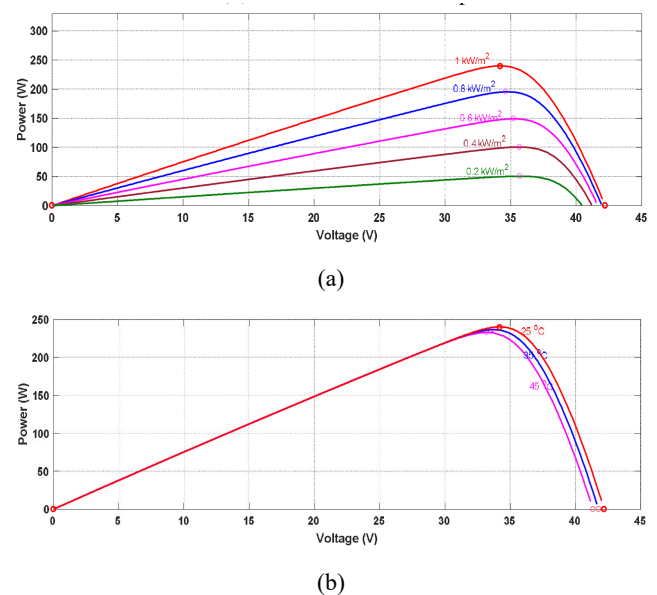
It is evident that there is only one maximum power point that changes with changes in solar irradiance and ambient temperature. It is important to operate the photovoltaic system at the maximum power point, so MPPT techniques are used to extract the maximum power from the photovoltaic system.

2.2 DC-DC converter

A boost converter is also called a step-up converter because its output voltage is always higher than the input voltage. Figure 6 shows the topology of the DC-DC boost converter. The boost converter consists of a voltage source, an

inductor, a capacitor, a diode, a switch, and the load resistance.

Figure 6   Boost converter topology
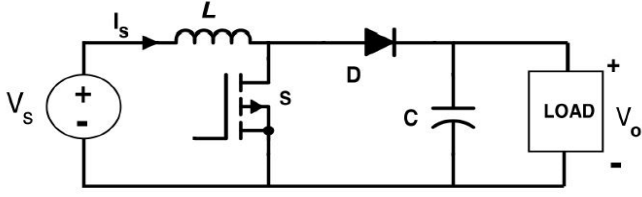
The switch (*S*) can be closed or opened to obtain the desired output voltage. The relationship between the input and output voltages is given in equation (4).

$$V_o = \frac{V_s}{1-D} \tag{4}$$

The inductor and capacitor values can be calculated using equations (5) and (6), respectively.

$$L_{min} = \frac{D(1-D)^2 R}{2f} \tag{5}$$

$$C_{min} = \frac{Dv_{rf}}{R} \tag{6}$$

where $v_r = \frac{\Delta V_o}{V_o}$.

The average inductor current can be obtained using the following equation:

$$I_L = \frac{V_s}{(1-D)^2 R} \tag{7}$$

Since the output voltage and the inductor current depend on the duty cycle, the working status of the boost converter can be controlled by adjusting the duty cycle. An MPPT technique is used to control this duty cycle and obtain the desired voltage. It is also used to get the boost converter to operate the photovoltaic system at the voltage, at which the maximum power point occurs.

3   Preliminary

The main drawback of the photovoltaic system is its low efficiency and high initial cost, and dependency on atmospheric conditions, as shown in Figures 4 and 5. Thus, the photovoltaic system has to be operated at its maximum power point under any atmospheric condition. MPPT techniques can be used to extract maximum power from a photovoltaic system irrespective of the atmospheric conditions. MPPT uses an electronic system to change the electrical operating point of the photovoltaic module to deliver maximum power. Figure 7 shows the schematic diagram of the photovoltaic system with MPPT technique.

Figure 7   Schematic diagram of MPPT (see online version for colours)
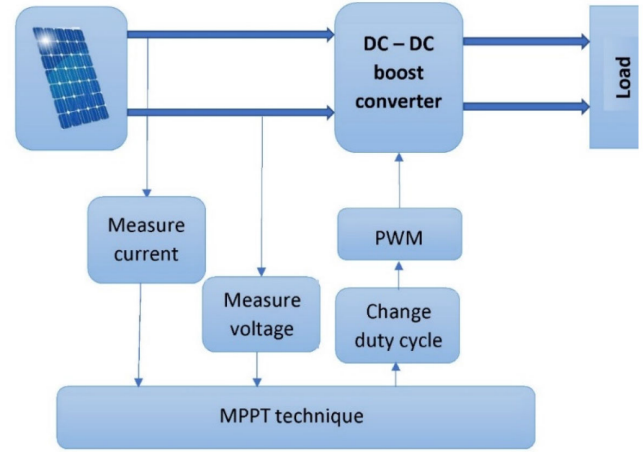
The MPPT techniques discussed can be classified as:

1   conventional

2   soft computing

3   optimisation-based MPPT techniques.

Under optimisation-based MPPT techniques, the PSO algorithm and CS algorithm are discussed, and they are compared with other conventional and soft computing techniques to prove that the PSO algorithm surpasses other techniques in performance.

In order to make the comparison, the conventional MPPT techniques (FSCC, FOCV, P&O and INC) techniques are recalled in this section. They are developed in former work in detail in Sher et al. (2015), Baimel et al. (2019), Elgendy et al. (2011) and Bollipo et al. (2020).

3.1   Fractional short circuit current

This technique depends on the linearity of the relationship between the current at which the maximum power point occurs (I_{MPP}) and the short circuit current (I_{sc}) (Sher et al., 2015). This linear relationship is presented in the following equation:

$$I_{MPP} \approx I_p I_{sc} \tag{8}$$

where I_p is the current proportional factor, which depends on the used photovoltaic panel. It will vary between 0.72 and 0.92.

The advantages of this method are its low cost – only one current sensor is required – simplicity, and ease of implementation. However, its efficiency is low because of the approximate relationship given in equation (8). Furthermore, it cannot track the maximum power point under changing atmospheric conditions. The flowchart of the FSCC technique is shown in Figure 8.

Figure 8 Flowchart of FSCC technique (see online version for colours)
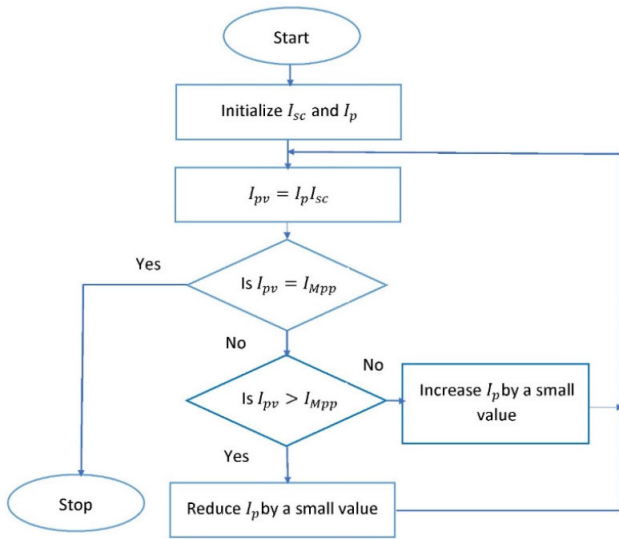
Figure 9 Flowchart of FOCV technique (see online version for colours)

Start

Initialize I_{sc} and I_p

$I_{pv} = I_p I_{sc}$

Is $I_{pv} = I_{Mpp}$

Yes → Stop

No

Is $I_{pv} > I_{Mpp}$

No → Increase I_p by a small value

Yes → Reduce I_p by a small value

Start

Initialize V_{oc} and V_p

$V_{pv} = V_p V_{oc}$

Is $V_{pv} = V_{Mpp}$

Yes → Stop

No

Is $V_{pv} > V_{Mpp}$

No → Increase V_p by a small value

Yes → Reduce V_p by a small value
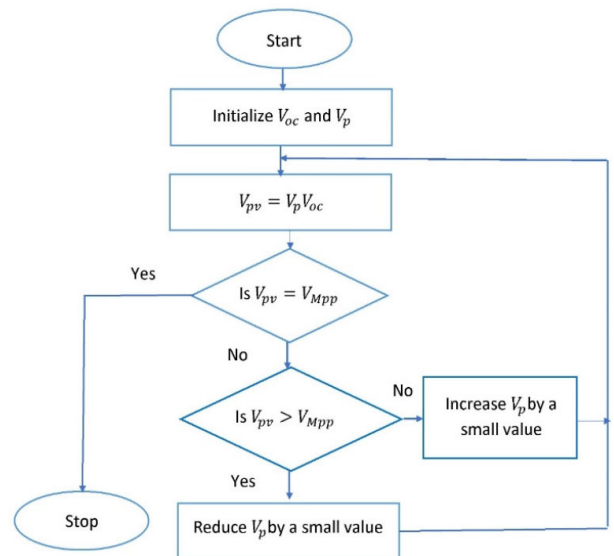
Figure 10 Flowchart of P&O technique (see online version for colours)

Start

Measure $I_{pv}(t-1)$, $V_{pv}(t-1)$

Calculate $P_{pv}(t-1) = I_{pv}(t-1) \times V_{pv}(t-1)$

Perturb the duty cycle of the converter

Measure $I_{pv}(t)$, $V_{pv}(t)$

Calculate $P_{pv}(t)$

$P_{pv}(t) > P_{pv}(t-1)$

Yes → $V_{pv}(t) > V_{pv}(t-1)$

Yes → $D(t) = D(t-1) + \Delta D$

No → $D(t) = D(t-1) - \Delta D$

No → $V_{pv}(t) > V_{pv}(t-1)$

Yes → $D(t) = D(t-1) - \Delta D$

No → $D(t) = D(t-1) + \Delta D$

Return
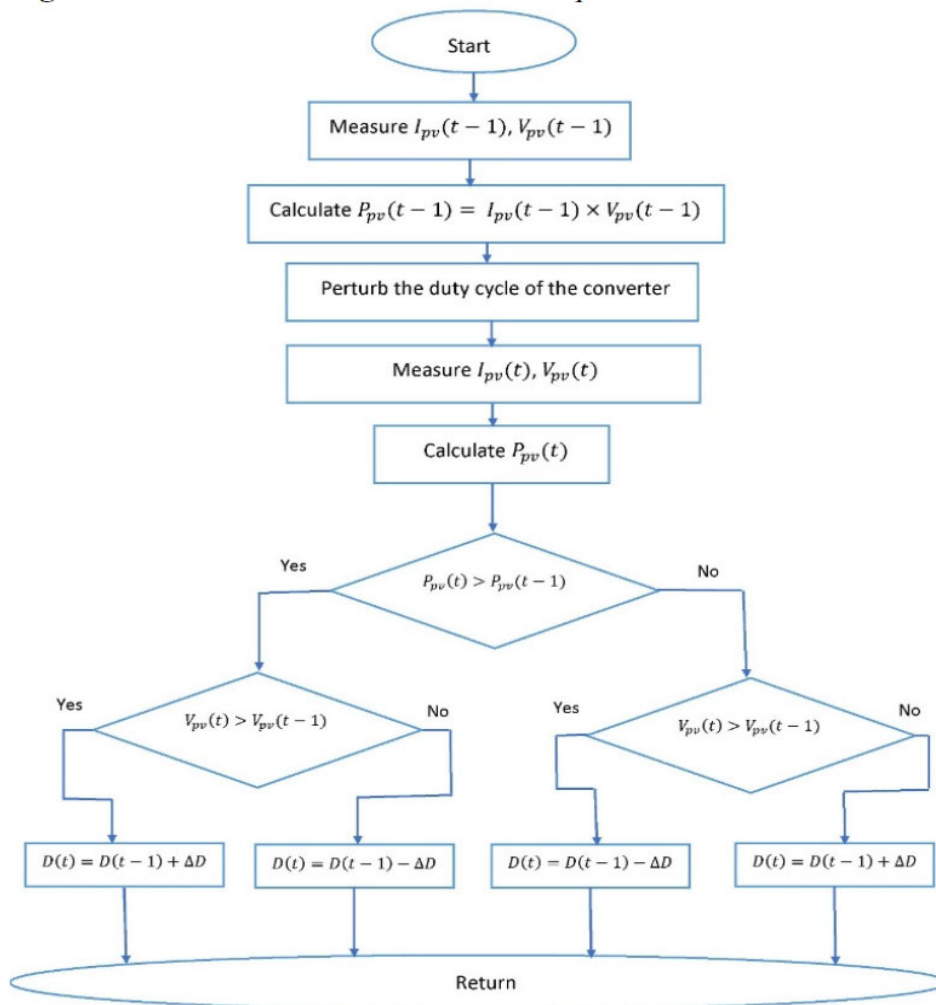
3.2 Fractional short circuit current

The FOCV technique is similar to the FSCC technique because it also depends on the linear relationship between the maximum power voltage (V_{MPP}) and the open-circuit voltage (V_{oc}) (Baimel et al., 2019), as shown in equation (9).

$$V_{MPP} \approx V_p V_{oc} \tag{9}$$

where V_p is the voltage proportional factor, which is unique to each photovoltaic module and provided in the module's datasheet. Its value is between 0.7 and 0.9. The flowchart of the FOCV technique is shown in Figure 9. This technique also has the same advantages and disadvantages as the FSCC technique.

3.3 Perturb and observe

The P&O technique is commonly used because of its simplicity and ease of implementation; it has only a few parameters to be measured. Figure 10 shows the flowchart of the P&O technique.

Figure 11 Maximum power point of the P-V curve (see online version for colours)
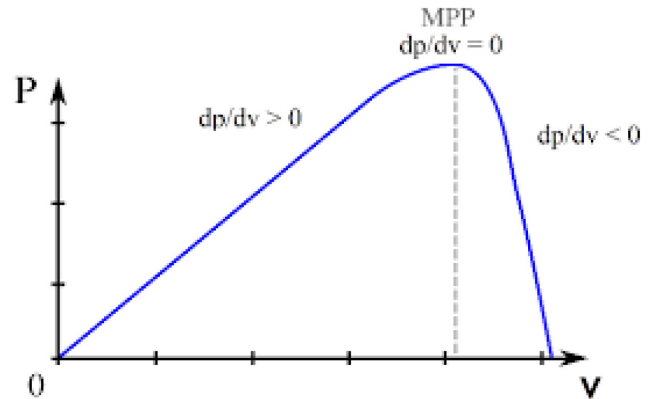
Figure 12 Flowchart of INC technique (see online version for colours)
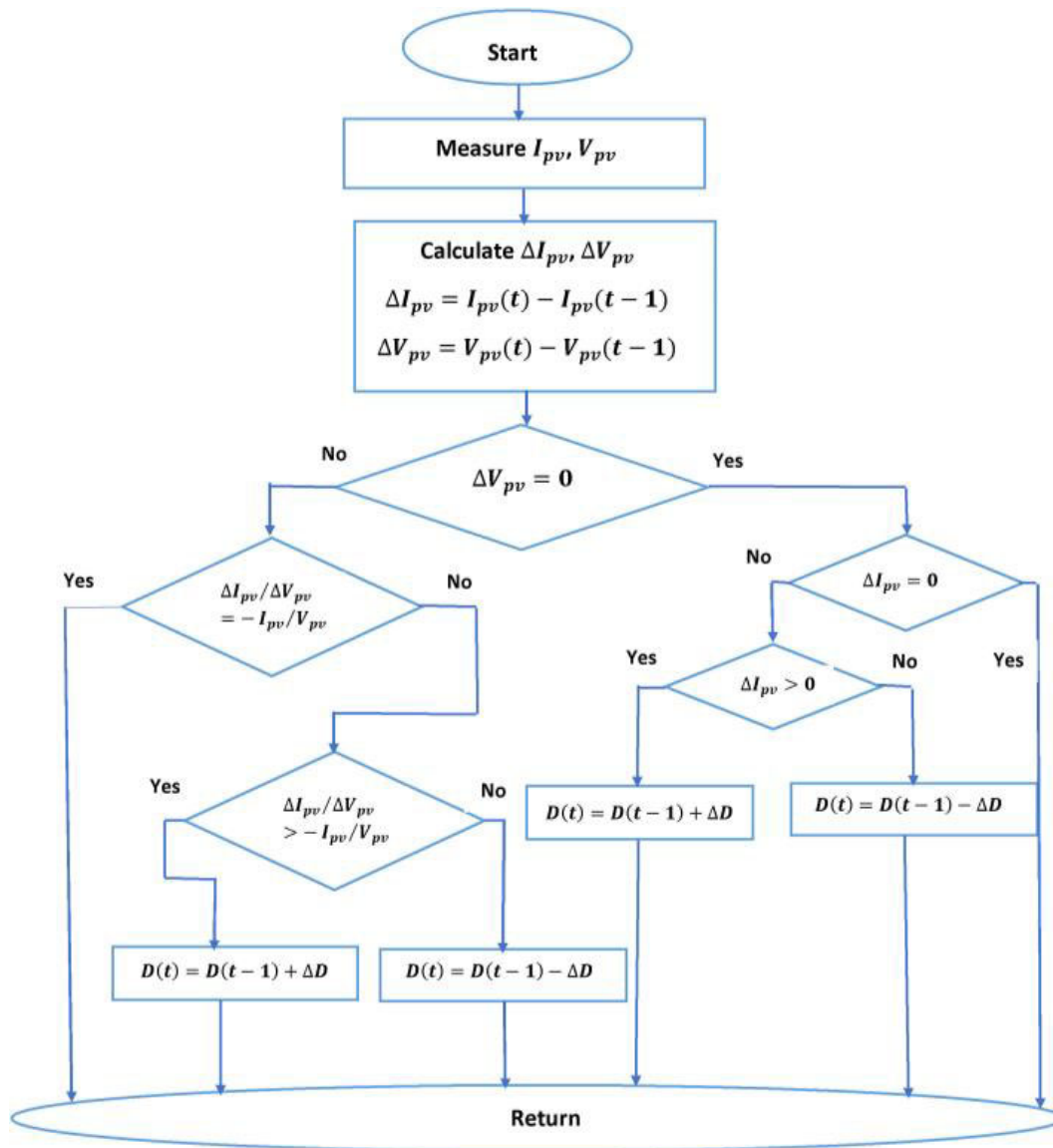
In this technique, the DC-DC converter duty cycle is periodically increased or decreased. The output parameters are measured after every perturbation, and the output power is computed. The computed output power at any given time is compared with its previous value, and if this previous value is less than the current value, the duty cycle would be perturbed in the same direction and vice versa (Elgendy et al., 2011).

The MPPT efficiency of the P&O technique is satisfactory. However, once the maximum power point is reached, the perturbations in the duty cycle will not cease, causing oscillations to occur around the maximum power point. The efficiency also depends on the step size ΔD. If ΔD has a low value, the convergence speed would be low; if its value is large, the oscillations will increase.

3.4 *Incremental conductance*

The INC technique is based on the fact that the derivative of the photovoltaic power with respect to the photovoltaic voltage is equal to zero at the maximum power point, as shown in Figure 11. It compares the instantaneous conductance with the INC as shown in the equations below.

At maximum power point

$$\frac{dP_{pv}}{dV_{pv}} = 0 \qquad (10)$$

$$\frac{dP_{pv}}{dV_{pv}} = \frac{d\left(I_{pv} \times V_{pv}\right)}{dV_{pv}} = 0 \qquad (11)$$

$$I_{pv} + V_{pv}\frac{dI_{pv}}{dV_{pv}} = 0 \qquad (12)$$

$$\frac{dI_{pv}}{dV_{pv}} = -\frac{I_{pv}}{V_{pv}} \qquad (13)$$

where $\dfrac{I_{pv}}{V_{pv}}$ is the instantaneous conductance and $\dfrac{dI_{pv}}{dV_{pv}}$ is INC.

According to equation (13), the maximum power point occurs when $\dfrac{dI_{pv}}{dV_{pv}} = -\dfrac{I_{pv}}{V_{pv}}$.

If the operating point is to the right of the maximum power point, then $\dfrac{dI_{pv}}{dV_{pv}} < -\dfrac{I_{pv}}{V_{pv}}$ and the photovoltaic voltage (V_{pv}) would decrease. If the operating point is to the left of the maximum power point, then $\dfrac{dI_{pv}}{dV_{pv}} > -\dfrac{I_{pv}}{V_{pv}}$ and the photovoltaic voltage (V_{pv}) would increase (Bollipo et al., 2020).

The flowchart of the INC technique is shown in Figure 12.

The INC technique, unlike the P&O technique, can cease when it reaches the maximum power point. Thus, although it does not cause oscillations around the maximum power point, its efficiency depends on the step size ΔD.

4 Proposed optimal MPPT techniques

4.1 *Fuzzy logic controllers*

FLCs have proved their ability in controlling nonlinear systems and are used in many applications (Qu et al., 2012). FLCs are used for tracking the maximum power points of photovoltaic systems because they can emulate human expert behaviour using knowledge gained from experience; they are also simple and reliable. Using an FLC, a nonlinear controller can be constructed using heuristic knowledge. Many past researchers have presented the basic principles of FLCs (Bai and Wang, 2006; Lee, 1990). The FLC process is shown in Figure 13.

Figure 13 FLC process (see online version for colours)
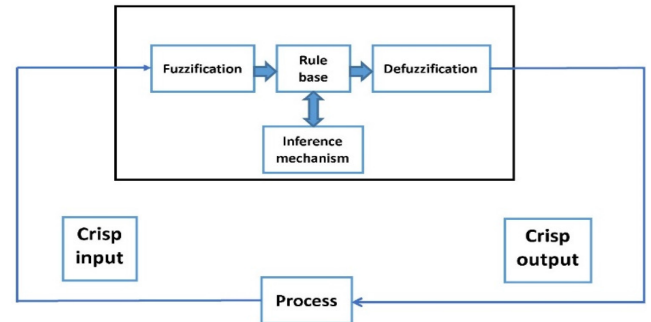
In the fuzzification step, the inputs to the controller are transformed from physical forms into fuzzy forms, and the degree of membership of a parameter can be determined by applying any fuzzy membership function, such as trapezoidal, triangular, Gaussian and sigmoid membership functions. The rule base step is represented by a group of if-then rules that represent heuristic knowledge. The inference mechanism decides whether the rules are appropriate to the current time. The defuzzification step converts the fuzzy controller output to a crisp signal to be processed.

In MPPT, the FLC inputs are the voltage change (ΔV_{pv}) and the power change (ΔP_{pv}) and the controlled signal is the DC-DC converter duty cycle change (ΔD). Five fuzzy sets are used to express the linguistic variables negative big (NEB), negative small (NES), zero (ZE), positive small (POS), and positive big (POB) for both the input and output variables of the designed controller. Table 1 presents the fuzzy rule base used to control the converter duty cycle. Figures 14, 15 and 16 show the Gaussian membership functions for the FLC inputs and outputs. The flowchart of the FLC-based MPPT technique is shown in Figure 17.

Table 1 Rule-base of the FLC

dp \ dv	NB	NS	ZE	PS	PB
NB	NS	NB	NB	PB	PS
NS	ZE	NS	NS	PS	ZE
ZE	ZE	ZE	ZE	ZE	ZE
PS	ZE	PS	PS	NS	ZE
PB	PS	PB	PB	NB	NS

Figure 14   Membership function for the voltage change ΔV_{pv} (see online version for colours)
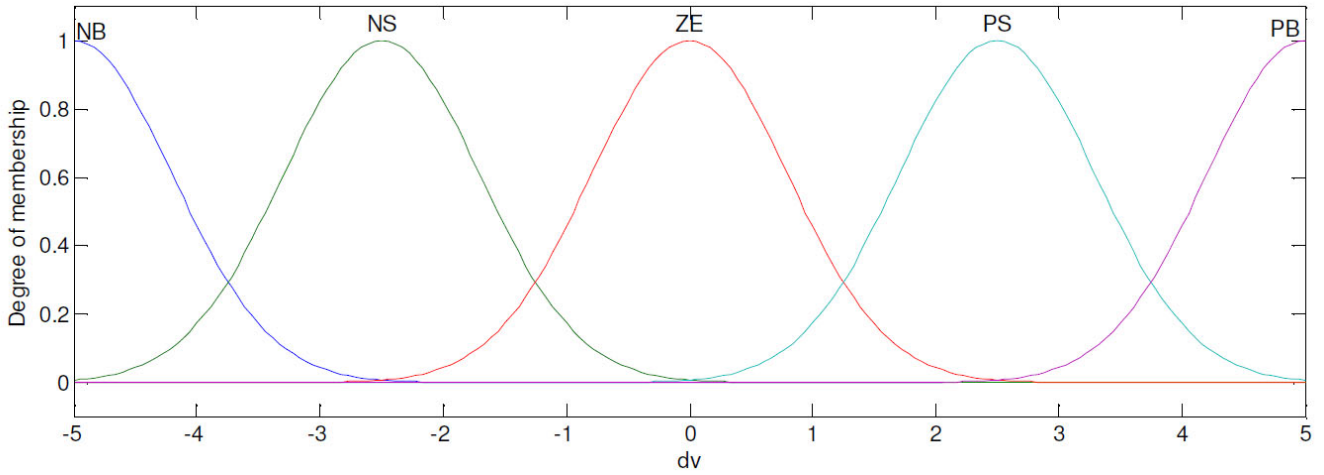
Figure 15   Membership function for the voltage change Δp_{pv} (see online version for colours)
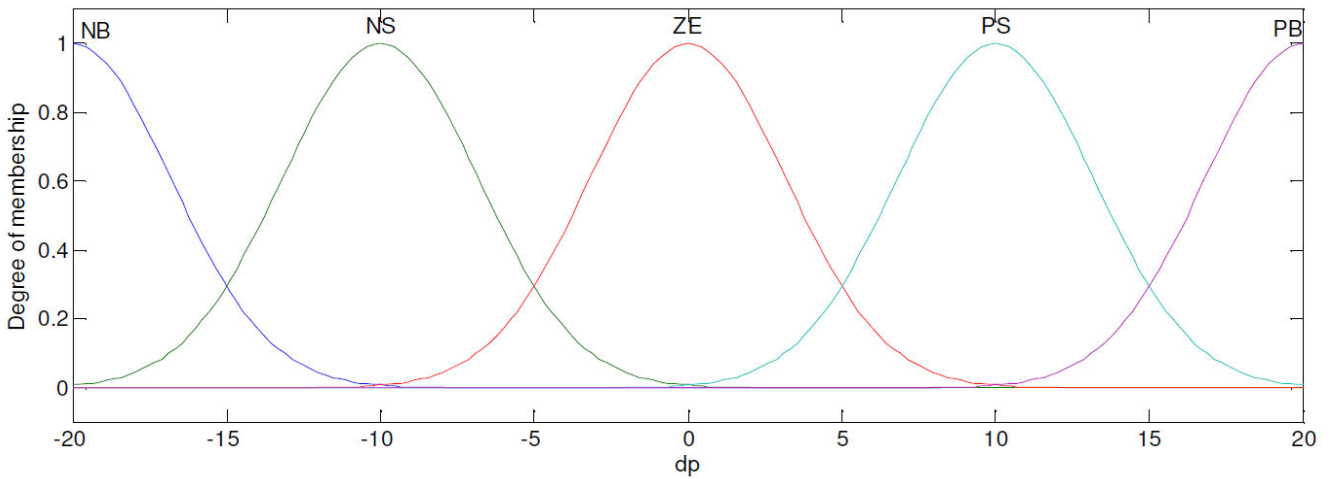
Figure 16   Membership function for the voltage change ΔD (see online version for colours)
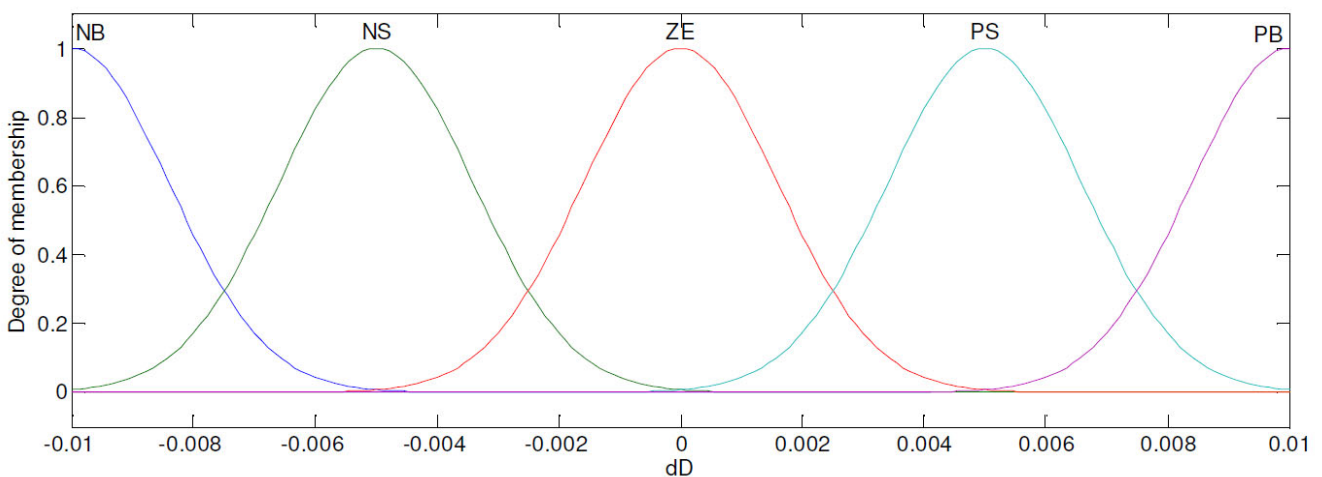
4.2   *Artificial neural network*

An ANN is a mathematical model used to mimic the structure and the functions of a biological neural network. ANN has proved its efficiency in controlling a nonlinear system in many applications (Sun and Zhu, 2012; Kankar et al., 2012; Bansal, 2009). The structure of an ANN can be represented by a group of neurons connected to process information. An ANN is an adaptive system that can change

its own structure based on internal or external information. ANNs can solve complicated problems encountered in control systems, signal processing and pattern recognition.

Figure 17 Flowchart of FLC-based MPPT technique (see online version for colours)
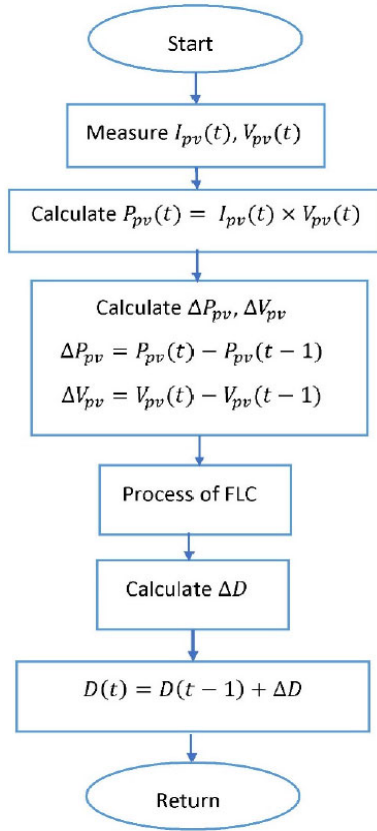
In the last decade, ANNs were used to extract maximum power from photovoltaic systems because of their self-learning capabilities and the ability to predict the maximum power points of the photovoltaic systems under different atmospheric conditions. The structure of an ANN is shown in Figure 18. It has three layers: input layer, hidden layer and output layer. The input layer consists of two neurons to represent the inputs of the ANN, the hidden layer of four neurons, and the output layer of one neuron to represent the ANN output.

In MPPT, the inputs of the ANNs are the photovoltaic voltage and power changes represented by X_1 and X_2, respectively and the output is the converter's duty cycle change (D) represented by U as shown in Figure 18. After calculating the duty cycle using the ANN technique, the photovoltaic output power (P_{opv}) is compared with the desired photovoltaic power (P_{dpv}) to calculate the error (e) which is used by the error back propagation tuning (EBPT) algorithm to adjust the weights of the hidden layer (w_{ij}, $i = 1, \ldots, 4, j = 1, 2$) and the weights of the output layer ($Vi, i = 1, \ldots, 4$).

4.3 NF controller

NF controllers have the advantages of both ANNs and FLCs but do not have the disadvantages of the latter two. The heuristic knowledge and commentary power of an FLC can be combined with the computational and learning ability of an ANN to form a transparent ANN and a competent FLC that learns from previous experience. NF controllers have proved their efficiency in controlling nonlinear systems in many applications (Singh et al., 2009; Yang and Zhao, 2012). An NF controller is illustrated in detail in Abdulaziz, et al. (2019). Figure 19 shows the NF network structure. The purpose and the tasks of each layer are given below:

- Layer 1 (input layer): This layer conveys the crisp input to the fuzzification layer

$$X_i^{(1)} = X_i, i = 1, 2, \ldots\ldots \tag{14}$$

where X represents the inputs of the NF network.

- Layer 2: The fuzzification process is performed in this layer to calculate the degree to which the crisp input matches the fuzzy membership function. The process can be described using equation (15) given below.

$$X_{ij}^{(2)} = \exp\left(-\frac{\left(X_i^{(1)} - c_{ij}\right)^2}{\sigma_{ij}^2}\right) \tag{15}$$

where c_{ij} and σ_{ij} represent the mean and the deviation of the Gaussian membership function, respectively, for the i_{th} dimension and j_{th} rule node.

- Layer 3: This is the rule node that calculates the firing strength by using the product operation shown below:

$$X_i^{(3)} = \prod_i X_{ij}^{(2)}. \tag{16}$$

- Layer 4: This is the defuzzification layer, which calculates the crisp output as shown below:

$$X_i^{(4)} = \left(\sum_{i=1}^m \sum_{z=1}^n X_i^{(3)} * O_z\right)\Big/ X_i^{(3)} \tag{17}$$

$z = 1, 2, \ldots\ldots, n$, where the number of output membership functions is denoted by n, and the centre of the output membership function is denoted by O_z.

In MPPT, the inputs of the NF controllers are the changes in the photovoltaic output voltage (ΔV_{pv}) and power (ΔP_{pv}) and the output is the change in the duty cycle (ΔD). When the duty cycle change (ΔD) is calculated using the NF controller, the actual photovoltaic output power (P_{opv}) is compared with the desired photovoltaic power (P_{dpv}) to adjust the NF parameters (i.e., width and deviation of the fuzzy membership function) using the EBPT algorithm described below.

Assuming a single output parameter, the EBPT algorithm distinguishes the objective function shown in equation (18).

$$E(d) = \frac{1}{2}\left(P_{ppv}(d) - P_{opv}(d)\right)^2 \tag{18}$$

where $E(d)$ is the error signal for the present iteration.

Figure 18   Structure of ANN (see online version for colours)
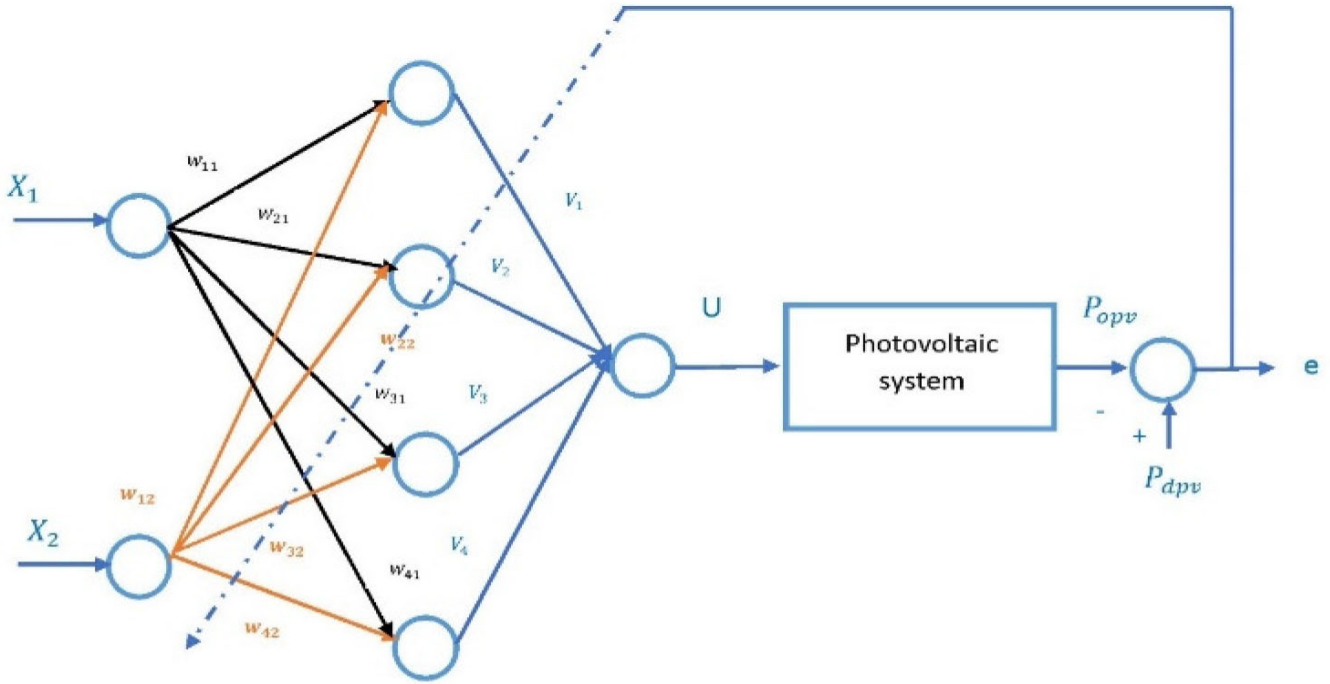
Figure 19   Structure of NF network (see online version for colours)
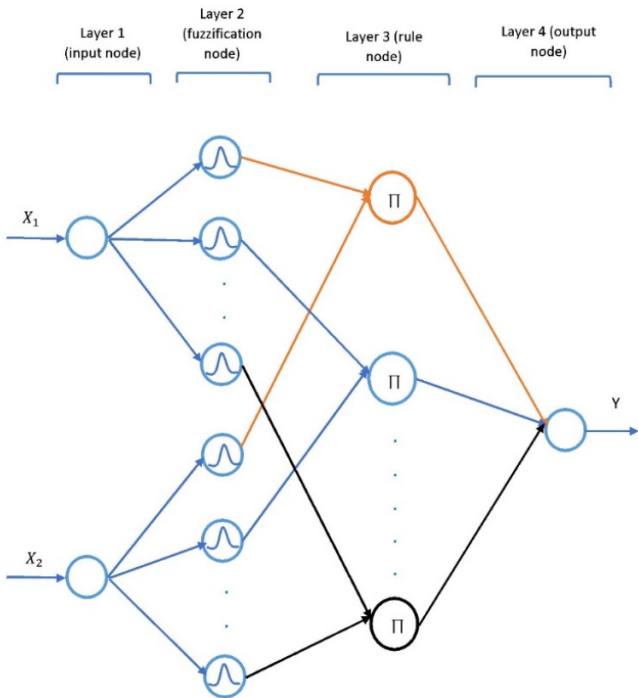
The centre of the output membership function in Layer 5 can be updated using the following equation:

$$O_z(d+1) = O_z(d) + \Delta O_z = O_z(d) - \eta \frac{\partial E}{\partial O_z}$$

$$= O_z(d) - \eta \frac{\partial E}{\partial Y} * \eta \frac{\partial Y}{\partial c_z} \tag{19}$$

where Y is the output of the NF network.

The following equations are used to update the parameters c_{ij} and σ_{ij} in Layer 2:

$$c_{ij}(d+1) = c_{ij}(d) - \eta \frac{\partial E}{\partial c_{ij}}$$

$$= c_{ij}(d) - \eta \left(\frac{\partial E}{\partial Y} * \frac{\partial Y}{\partial D_i^{(3)}} * \frac{\partial D_i^{(3)}}{\partial D_i^{(2)}} * \frac{\partial D_i^{(2)}}{\partial c_{ij}} \right) \tag{20}$$

$$\sigma_{ij}(d+1) = \sigma_{ij}(d) - \eta \frac{\partial E}{\partial \sigma_{ij}}$$

$$= \sigma_{ij}(d) - \eta \left(\frac{\partial E}{\partial Y} * \frac{\partial Y}{\partial D_i^{(3)}} * \frac{\partial D_i^{(3)}}{\partial D_i^{(2)}} * \frac{\partial D_i^{(2)}}{\partial \sigma_{ij}} \right) \tag{21}$$

where $\eta < 1$ is the learning constant.

4.4   PSO-based MPPT techniques

Swarm-based algorithms can solve complex problems because they can cover a wide range of applications owing to their robustness, ease of implementation, low cost and flexibility (Huynh and Dunnigan, 2012; Shivakumar et al., 2012). PSO is a swarm-based algorithm introduced by Kennedy and Eberhart (1995). PSO is used in many applications because it is accurate, reliable, and easy to implement, requires only a small calculational memory, and has only a few lines of code and parameters to be determined. PSO is inspired by a biological herd of birds seeking food in a specific area. In PSO, the herd is called the 'swarm', and the birds are called 'particles'. Firstly, the swarm is initialised in the search space with several particles in random positions. These particles search for the optimum solution. The position and velocity of each particle

are updated after each iteration, based on the following equations (Poli et al., 2007):

$$v_i(t+1) = \omega(t+1) * v_i(t) + C_1 r_1 \left(p_{best} - p_i(t) \right) + C_2 r_2 \left(g_{best} - p_i(t) \right) \tag{22}$$

$$p_i(t+1) = p_i(t) + v_i(t+1) \tag{23}$$

where $v_i(t+1)$ is the current velocity, $v_i(t)$ the previous velocity, $p_i(t+1)$ the current position, $p_i(t)$ the previous position of the particle i, and r_1 and r_2 are random numbers where $r_1, r_2 \in [0, 1]$, C_1 and C_2 are the cognitive learning rates, $\omega(t+1)$ is the inertia weight in the current iteration, p_{best} is the best position achieved by the particle, and g_{best} is the best position achieved by the particle neighbours.

After updating the position and velocity of each particle, the fitness evaluation function is calculated. If the fitness value of the updated particle is better than the memorised personal best position (p_{best}), p_{best} is adjusted to make it equal to the position of the current particle, and the same procedure is repeated for the global best position (g_{best}). The flowchart of the PSO algorithm is shown in Figure 20.

Figure 20 Flowchart of PSO algorithm
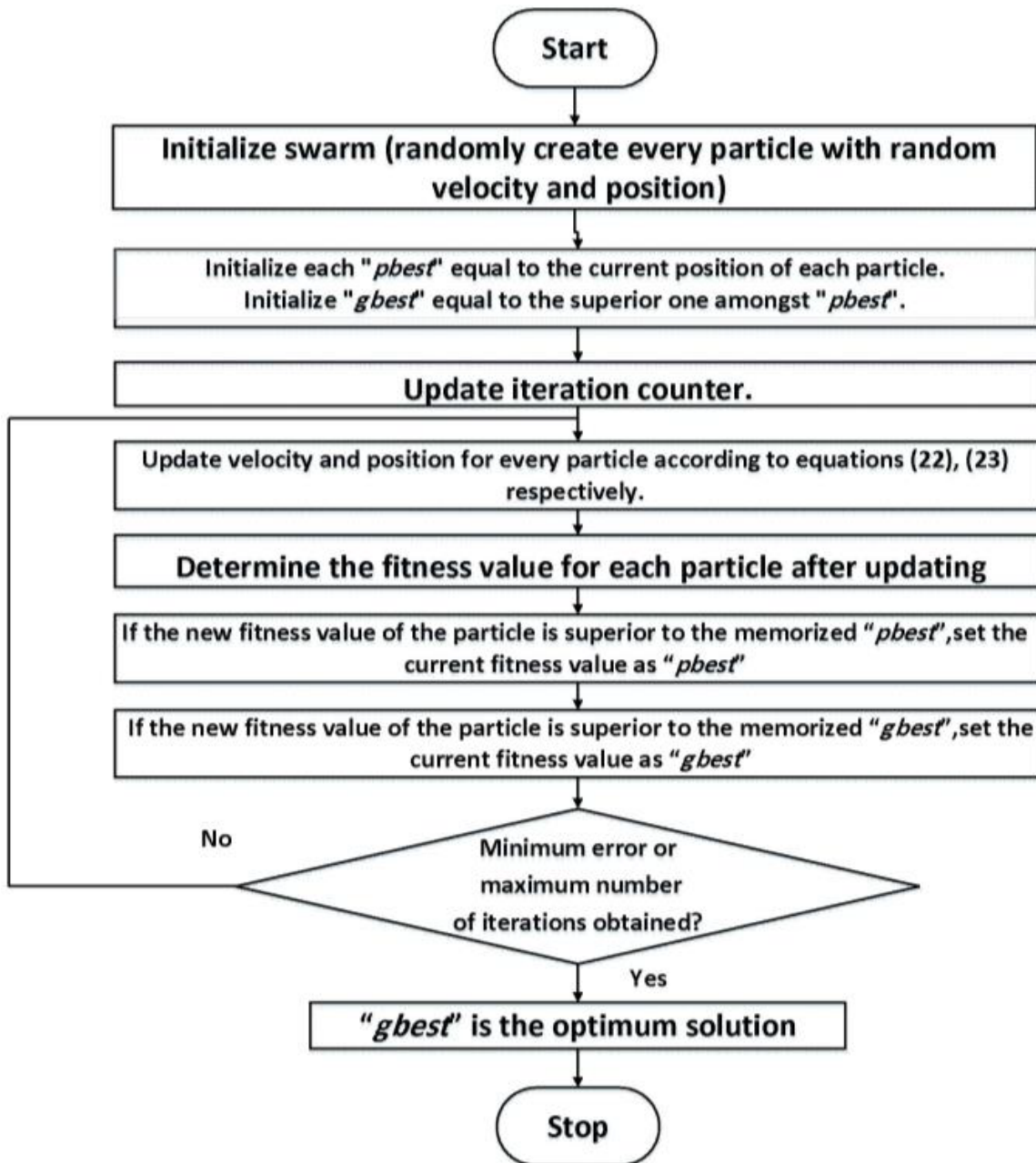
Figure 21   Pseudo-code of the CS algorithm

```
Begin

    Generate initial population (n) host nests and assign the position of each nest
    x_i^(t), i = 1,2,......,n, initialize p_a = 0.25.

        While (iter ≤ iter_max)
            Get a nest randomly using Lévy flight.
            Evaluate its fitness F(x_i^(t)).
            Randomly choose a nest (j) among the population and evaluate its
            fitness F(x_j^(t)).

                If F(x_i^(t)) > F(x_j^(t))
                    Replace x_j^(t) by x_i^(t+1) using equation (25)
                End (if)

            A fraction p_a of worst nests occurs.
            Worst nests are abounded and new nests are built.
            Keep the best solutions with higher fitness values.
            Rank the solutions and find the current best solution.
            Set iter = iter + 1.
        End (while)

    Find the best solution.
End
```

According to equation (22), the velocity of the current particle is affected by many parameters, such as ω, C_1, C_2, r_1 and r_2. Therefore, they have to be carefully chosen to obtain the globally optimal solution and avoid a local optimal solution.

In order to avoid falling in local optimal solution, the inertia weight for each iteration can be obtained using the following equation:

$$\omega_{iter} = \omega_{max} - \frac{\omega_{max} - \omega_{min}}{iter_{max}} * iter \qquad (24)$$

where ω_{max} is the maximum inertia weight ($\omega_{max} = 0.9$), ω_{min} is the minimum inertia weight ($\omega_{min} = 0.4$), $iter_{max}$ is the maximum number of iterations, and $iter$ is the current iteration number. According to this equation, the inertia weight (ω) will be at its maximum value at the start of the iterations in order to accelerate the particles' velocity and reach the optimal solution as quickly as possible. The value of (ω) will be reduced at the end of iterations to ensure that the global optimal solution is reached.

C_1 and C_2 have to be adjusted because if C_1 is larger than C_2, the algorithm would be stuck in the local optimal solution rather than the globally optimal solution. If C_2 is larger than C_1, the result would be an extreme movement in the search space (He et al., 2016). As a result, the values of all the parameters should be carefully chosen to obtain the globally optimal solution.

In MPPT, the particle position represents the converter's duty cycle, while the fitness evaluation function represents the photovoltaic generated power. The PSO algorithm in MPPT has the following steps:

Step 1   Initialisation step – In this step, a swarm is initialised with several particles placed at fixed positions and covering the search space. The search space extends from D_{max} to D_{min} where D_{max} and D_{min} are the maximum and minimum duty cycles of the converter, respectively.

Step 2   Fitness evaluation – After calculating the converter's duty cycle, the photovoltaic generated current (I_{pv}) and voltage (V_{pv}) are measured to calculate the photovoltaic power (P_{pv}). The photovoltaic power is the fitness function, and the PSO algorithm has to maximise its value.

Step 3   Updating the personal and global best position – If the fitness value of the particle is greater than its memorised value, (p_{best}) has to be updated to make it equal to the current particle's position, and the same procedure has to be followed for (g_{best}).

Step 4   Updating – The velocity and position of each particle has to be updated according to equations (22) and (23), respectively.

Step 5 Repeating – The previous steps have to be repeated until the generated photovoltaic output power (P_{opv}) is equal to the desired photovoltaic power (P_{dpv}) or the maximum number of iterations is reached.

4.5 CS algorithm

Yang and Deb (2009) developed the CS algorithm. It is a metaheuristic algorithm inspired by the breeding strategy of cuckoo birds. Cuckoo birds lay their own eggs on other birds' nests; these birds are called host birds. To increase the reproduction probability of their own eggs, cuckoo birds may throw away the host birds' eggs. Cuckoo eggs are often very similar to host eggs except that they are slightly bigger. Cuckoo eggs are hatched earlier than host eggs, and once the cuckoo chick is hatched, it will expel the host eggs from the nest to increase its feeding chance. The host bird can discover the cuckoo eggs with probability p_a where $p_a \in [0, 1]$. When the host bird discovers cuckoo eggs, it will either destroy them or abandon the nest and build another one.

Looking for the host nests is similar to the process of searching for food. It is found that *Drosophila melanogaster* fruit flies search the landscape using a sequence of straight forward flight directions interrupted by a rapid 90° shift which leads to the Lévy flight style (Reynolds and Frye, 2007).

Figure 22 Flowchart of CS algorithm
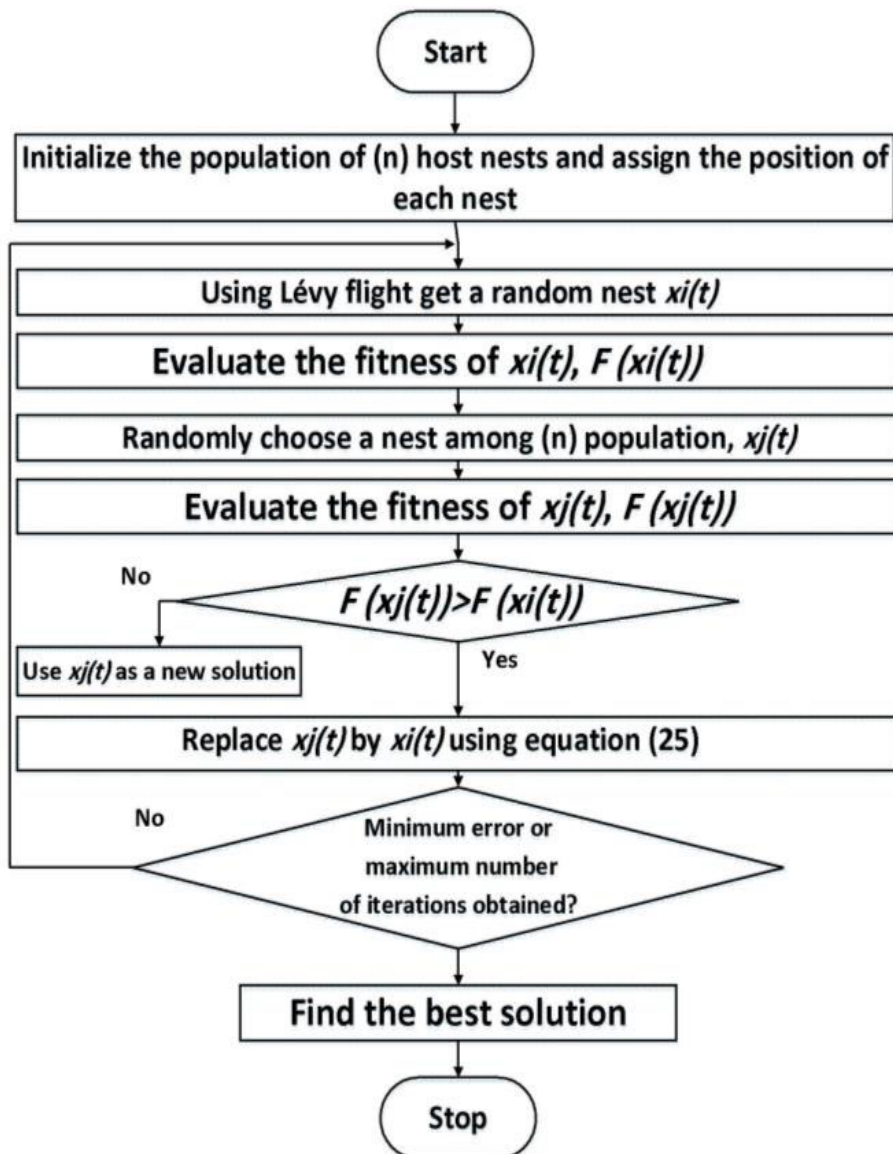
The eggs in the nest refer to a set of solutions in the CS algorithm, and the cuckoo egg is the new solution. There are three main rules:

1 The cuckoo bird lays only one egg at a time in a randomly selected nest.

2 The nest with eggs similar to the host egg is the best nest and will carry over to the next generation.

3 The number of nests is fixed, and the probability that the host bird discovers the cuckoo egg is $p_a \in [0, 1]$. This is the worst solution, and the nest will be replaced in the next generation by randomly generated nests with random solutions.

The new nests are generated by the Lévy flight equation as shown below:

$$x_i^{(t+1)} = x_i^{(t)} + \alpha \oplus L\acute{e}vy(\lambda) \qquad (25)$$

where $x_i^{(t+1)}$ is the new solution, $x_i^{(t)}$ is the current solution, α is the step size and $\alpha > 0$, $\oplus$ is entry wise multiplication, and $L\acute{e}vy(\lambda)$ can be obtained by the following equation:

$$L\acute{e}vy(\lambda) \approx u = l^{-\lambda} \qquad (26)$$

where $1 < \lambda < 3$.

For further explanation of the CS algorithm steps, it is explained in pseudo-code and flowchart in Figures 21 and 22, respectively.

In MPPT, the nest position represents the converter's duty cycle, while the fitness evaluation function represents the photovoltaic generated power.

5   Simulation results

MSX-60 photovoltaic module was built using MATLAB/Simulink program to analyse the performance of the MPPT techniques. The specifications of the MSX-60 photovoltaic module are presented in Table 2. The simulation was done for different solar irradiance levels with the temperature fixed at 25°C.

Table 2   Specification of MSX-60 module

No. of cells per module	36
Open circuit voltage	21.8 V
Short circuit current	3.8 A
Voltage at the maximum power point	17.1 V
Current at the maximum power point	3.5 A
Open circuit voltage temperature coefficient	–0.08 V/°C
Short circuit current temperature coefficient	0.003 A/°C
No. of series connected modules	2
No. of parallel connected modules	2
Maximum power point	59.85 W

5.1   Constant solar irradiance

In this case, the solar irradiance is maintained at 1,000 W/m². The photovoltaic generated power for each technique is shown in Figure 23.

5.2   Gradually changing solar irradiance

The solar irradiance is changed gradually from 700 to 1,000 W/m², as shown in Figure 24. The performance of each technique is shown in Figure 25.

5.3   Rapidly changing solar irradiance

The solar irradiance is unstable and changes rapidly from 550 to 1,000 W/m², as shown in Figure 26.

Figure 27 shows the photovoltaic generated power using different MPPT techniques.

Figures 23, 25 and 27 indicate that the FSCC and FOCV techniques cannot track the maximum power point, even when the solar irradiance is constant. The P&O technique has acceptable performance and fast response, although it continuously oscillates around the maximum power point. INC also has acceptable performance but slightly oscillates around the maximum power point. It is obvious that the P&O and INC techniques take some time to reach the maximum power point, at the beginning of iterations, but they reach to the maximum power point very fast in case of rapid transition of the solar irradiance.

Figure 23   Performance of different MPPT techniques under constant atmospheric conditions
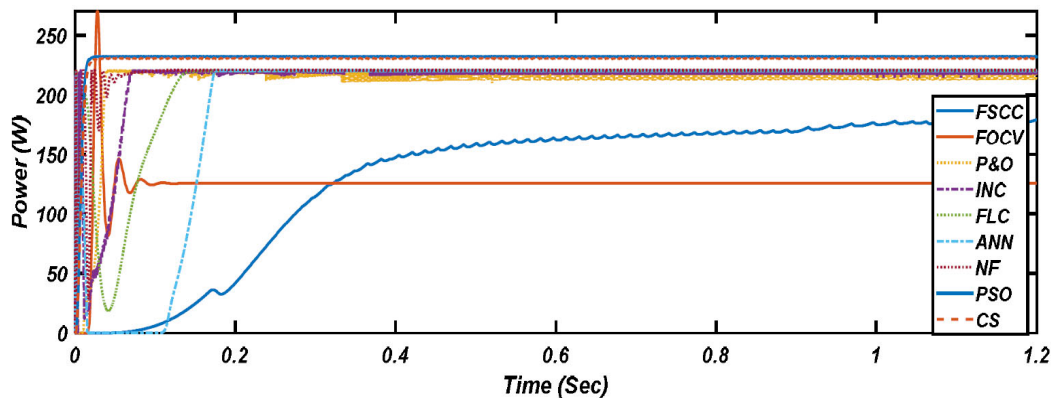
Figure 24 Solar irradiance vs. time (see online version for colours)
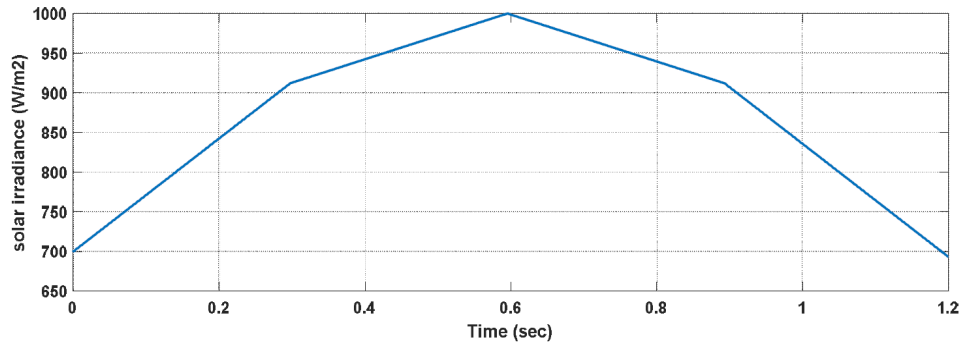
Figure 25 Performance of different MPPT techniques under gradually changing solar irradiance (see online version for colours)
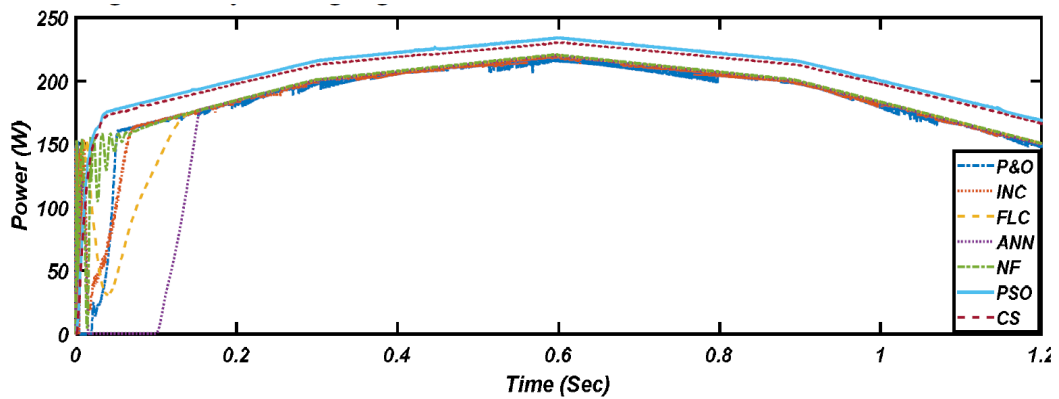
Figure 26 Solar irradiance vs. time (see online version for colours)
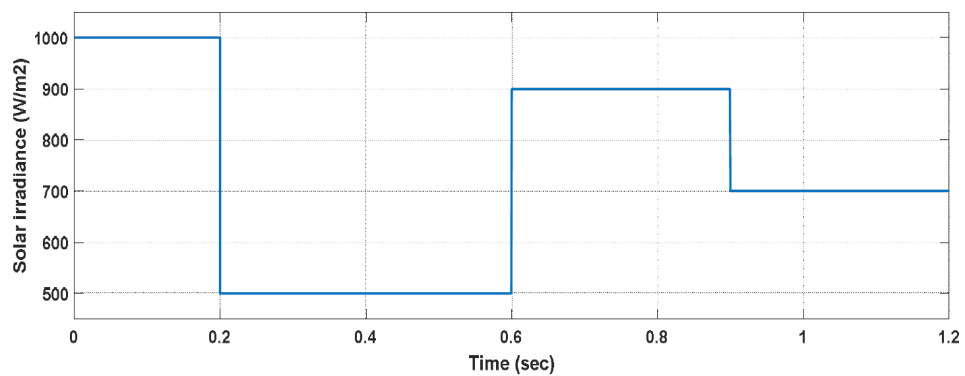
Figure 27 Performance of different MPPT techniques under rapidly changing solar irradiance (see online version for colours)
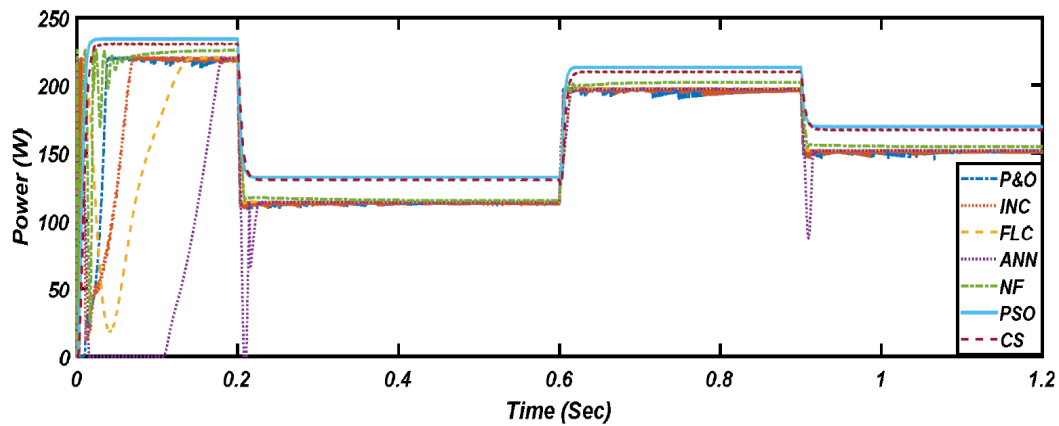
Figure 28   Partial shading conditions scenario (see online version for colours)

Figure 29   Performance of different MPPT techniques under partial shading conditions (see online version for colours)
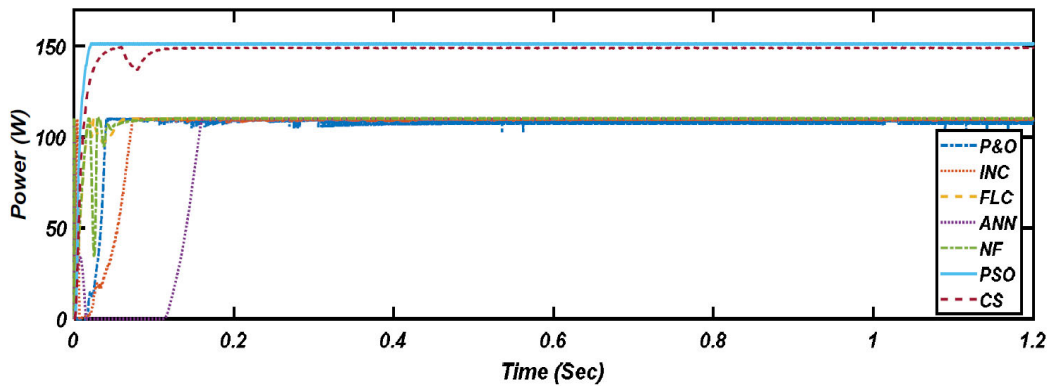
The FLC technique has satisfactory performance with no oscillation at all; however, it takes a long time to track the maximum power point. The ANN technique also has satisfactory performance with no oscillations, but it takes a long time to yield output. The performance of the NF technique is better than the performance of any of the other techniques already mentioned, but it has slight oscillations at the beginning of iterations. It is also clear that the soft computing techniques take a while to reach the maximum power point, in case of rapid change in solar irradiance.

The CS and PSO techniques have the best performance under any atmospheric condition because they can track the optimum maximum power point efficiently and robustly, but the performance of the PSO algorithm is slightly faster and better than the performance of the CS algorithm. It is obvious that the CS and PSO techniques have the fastest response at the beginning of iterations and acceptable convergence speed during rapidly changing solar irradiance. However, conventional techniques have a faster response under rapidly changing solar irradiance.

5.4 Partial shading conditions

The photovoltaic array is tested under partial shading condition scenario, as shown in Figure 28. The performance of each MPPT technique is shown in Figure 29.

Figure 29 indicates that the conventional and soft computing techniques failed to track the maximum power point, under partial shading conditions. It is evident that the CS and PSO algorithms can track the maximum power point efficiently, under partial shading conditions, but the performance of the CS algorithm is not stable at the beginning of iterations. Table 3 shows comparisons in performance between the discussed MPPT techniques.

Table 3   Performance comparison of MPPT techniques

Technique	Efficiency (%)	Computational complexity	Convergence speed
FSCC	67.23%	Simple	Low
FOCV	53.67%	Simple	Medium
P&O	93.32%	Simple	High
INC	93.86%	Simple	High
FLC	94.12%	Simple	Medium
ANN	94.08%	Simple	Medium
NF	94.34%	Medium	Medium
PSO	99.14%	Medium	High
CS	98.46%	Medium	High

6 Conclusions

In this paper, conventional, soft computing, and optimisation-based MPPT techniques were discussed and applied to a photovoltaic system using the MATLAB/Simulink program, to determine the performance of each technique under changing atmospheric conditions. Simulation results indicate that the FSCC and FOCV techniques cannot reach the maximum power point and their tracking efficiency is low. The tracking efficiency of the P&O technique is acceptable, and it can quickly reach the steady-state. The efficiency of the INC technique is better than that of the P&O technique, but the P&O technique still displays a faster response than INC. Soft computing techniques are more efficient than conventional techniques, but they take a long time to reach the steady-state. The NF technique is the most efficient soft computing technique. The performance of the CS algorithm is better than the

performance of any of the other techniques already mentioned. The PSO algorithm is superior in performance to others because it can robustly and efficiently track the maximum power point, with a fast response. However, it takes a long execution time, and its response is slightly slower than that of conventional techniques under rapidly changing solar irradiance. It is expected that researchers will work to develop a new technique that combines between the convergence speed of conventional techniques under rapidly changing atmospheric conditions and the efficiency of the PSO technique, to further track the maximum power point more efficiently.

References

Abdulaziz, S., Nabil, E., Zaki, G. and Atlam, G. (2019) 'Tuning the parameters of TSK neuro-fuzzy system by particle swarm optimization', *Menoufia Journal of Electronic Engineering Research*, Vol. 28, No. 2, pp.245–258.

Abido, M.A., Khalid, M.S. and Worku, M.Y. (2015) 'An efficient ANFIS-based PI controller for maximum power point tracking of PV systems', *Arabian Journal for Science and Engineering*, Vol. 40, No. 9, pp.2641–2651.

Abouadane, H., Fakkar, A., Elkouari, Y. and Ouoba, D. (2017) 'Performance of a new MPPT method for photovoltaic systems under dynamic solar irradiation profiles', *Energy Procedia*, Vol. 142, pp.538–544.

Ahmad, J. (2010) 'A fractional open circuit voltage based maximum power point tracker for photovoltaic arrays', in *2010 2nd International Conference on Software Technology and Engineering*, IEEE, October, Vol. 1, pp.51–247.

Ahmed, J. and Salam, Z. (2013) 'A soft computing MPPT for PV system based on cuckoo search algorithm', in *4th International Conference on Power Engineering, Energy and Electrical Drives*, IEEE, May, pp.558–562.

Alexandru, C. (2019) 'Multi-body system simulation of the sun trackers used for PV panels', in *IOP Conference Series: Materials Science and Engineering*, IOP Publishing, August, Vol. 568, No. 1, p.012001.

Bai, Y. and Wang, D. (2006) 'Fundamentals of fuzzy logic control – fuzzy sets, fuzzy rules and defuzzifications', in *Advanced Fuzzy Logic Technologies in Industrial Applications*, pp.17–36, Springer, London.

Baimel, D., Tapuchi, S., Levron, Y. and Belikov, J. (2019) 'Improved fractional open circuit voltage MPPT methods for PV systems', *Electronics*, Vol. 8, No. 3, p.321.

Bansal, R.C. (2009) 'ANN based reactive power control of isolated wind-diesel-micro-hydro hybrid power systems', *International Journal of Modelling, Identification and Control*, Vol. 6, No. 3, pp.196–204.

Bollipo, R.B., Mikkili, S. and Bonthagorla, P.K. (2020) 'Critical review on PV MPPT techniques: classical, intelligent and optimisation', *IET Renewable Power Generation*, Vol. 14, No. 9, pp.1433–1452.

Camacho, E.F., Berenguel, M., Alvarado, I. and Limon, D. (2010) 'Control of solar power systems: a survey', *IFAC Proceedings Volumes*, Vol. 43, No. 5, pp.817–822.

Chim, C.S., Neelakantan, P., Yoong, H.P. and Teo, K.T.K. (2011) 'Fuzzy logic based MPPT for photovoltaic modules influenced by solar irradiation and cell temperature', in *2011 UkSim 13th International Conference on Computer Modelling and Simulation*, IEEE, March, pp.376–381.

Dahmane, M., Bosche, J., El-Hajjaji, A. and Pierre, X. (2013) 'MPPT for photovoltaic conversion systems using genetic algorithm and robust control', in *2013 American Control Conference*, IEEE, June, pp.6595–6600.

Dolara, A., Faranda, R. and Leva, S. (2009) 'Energy comparison of seven MPPT techniques for PV systems', *Journal of Electromagnetic Analysis and Applications*, Vol. 1, No. 3, pp.152–162.

Douiri, M.R. (2019) 'A predictive model for solar photovoltaic power based on computational intelligence technique', *Arabian Journal for Science and Engineering*, Vol. 44, No. 8, pp.6923–6940.

Elgendy, M.A., Zahawi, B. and Atkinson, D.J. (2011) 'Assessment of perturb and observe MPPT algorithm implementation techniques for PV pumping applications', *IEEE Transactions on Sustainable Energy*, Vol. 3, No. 1, pp.21–33.

Elobaid, L.M., Abdelsalam, A.K. and Zakzouk, E.E. (2012) 'Artificial neural network based maximum power point tracking technique for PV systems', in *IECON 2012 –38th Annual Conference on IEEE Industrial Electronics Society*, IEEE, October, pp.937–942.

Eltamaly, A.M. and Abdelaziz, A.Y. (Eds.) (2019) *Modern Maximum Power Point Tracking Techniques for Photovoltaic Energy Systems*, pp.31–63, Springer.

Ezinwanne, O., Zhongwen, F. and Zhijun, L. (2017) 'Energy performance and cost comparison of MPPT techniques for photovoltaics and other applications', *Energy Procedia*, Vol. 107, No. 156, pp.297–303.

Feroz Mirza, A., Mansoor, M., Ling, Q., Khan, M.I. and Aldossary, O.M. (2020) 'Advanced variable step size incremental conductance MPPT for a standalone PV system utilizing a GA-tuned PID controller', *Energies*, Vol. 13, No. 16, p.4153.

Figueiredo, S.N., Aquino, R.N. and Zurita, M.E. (2019) 'Comparison between P&O-based and PSO-based MPPT algorithms for photovoltaic system under partially shaded conditions', in *2019 6th International Conference on Control, Decision and Information Technologies (CoDIT)*, IEEE, April, pp.685–690.

Gonzalez-Longatt, F.M. (2005) 'Model of photovoltaic module in Matlab', *2Do Congreso Iberoamericano de Estudiantes de Ingenieria Electrica, Electronica Ycomputacion (II CIBELEC Espagna)*.

He, Y., Ma, W.J. and Zhang, J.P. (2016) 'The parameters selection of PSO algorithm influencing on performance of fault diagnosis', in *MATEC Web of Conferences*, EDP Sciences, Vol. 63, p.02019.

Hiyama, T. and Kitabayashi, K. (1997) 'Neural network based estimation of maximum power generation from PV module using environmental information', *IEEE Transactions on Energy Conversion*, Vol. 12, No. 3, pp.241–247.

Huynh, D.C. and Dunnigan, M.W. (2012) 'Advanced particle swarm optimisation algorithms for parameter estimation of a single-phase induction machine', *International Journal of Modelling, Identification and Control*, Vol. 15, No. 4, pp.227–240.

Ilyas, M., Tanweer, S.M. and Rahman, A. (2013) 'Optimal placement of distributed generation on radial distribution system for loss minimisation & improvement of voltage profile', *International Journal of Modern Engineering Research (IJMER)*, Vol. 3, No. 4, pp.2296–2312.

Kankar, P.K., Sharma, S.C. and Harsha, S.P. (2012) 'Vibration-based fault diagnosis of a rotor bearing system using artificial neural network and support vector machine', *International Journal of Modelling, Identification and Control*, Vol. 15, No. 3, pp.185–198.

Kennedy, J. and Eberhart, R. (1995) 'Particle swarm optimization', in *Proceedings of ICNN'95 – International Conference on Neural Networks*, IEEE, November, Vol. 4, pp.1942–1948.

Labeeb, K., Shankar, S. and Ramprabhakar, J. (2016) 'Hybrid MPPT controller for accurate and quick tracking', in *2016 IEEE International Conference on Recent Trends in Electronics, Information & Communication Technology (RTEICT)*, IEEE, May, pp.1533–1537.

Lee, C.C. (1990) 'Fuzzy logic in control systems: fuzzy logic controller. I', *IEEE Transactions on Systems, Man, and Cybernetics*, Vol. 20, No. 2, pp.404–418.

Mohanty, S., Subudhi, B. and Ray, P.K. (2015) 'A new MPPT design using grey wolf optimization technique for photovoltaic system under partial shading conditions', *IEEE Transactions on Sustainable Energy*, Vol. 7, No. 1, pp.181–188.

Padmanaban, S., Priyadarshi, N., Bhaskar, M.S., Holm-Nielsen, J.B., Ramachandaramurthy, V.K. and Hossain, E. (2019) 'A hybrid ANFIS-ABC based MPPT controller for PV system with anti-islanding grid protection: experimental realization', *IEEE Access*, Vol. 7, pp.103377–103389.

Poli, R., Kennedy, J. and Blackwell, T. (2007) 'Particle swarm optimization – an overview', *Swarm Intelligence*, Vol. 1, No. 1, pp.33–57.

Qu, S., Tian, Y., Chen, C. and Ai, L. (2012) 'A small intelligent car system based on fuzzy control and CCD camera', *International Journal of Modelling, Identification and Control*, Vol. 15, No. 1, pp.48–54.

Rajavel, A. and Prabha, N.R. (2020) 'Fuzzy logic controller-based boost and buck-boost converter for maximum power point tracking in solar system', *Transactions of the Institute of Measurement and Control*, Vol. 43, No. 4, pp.945–957.

Reynolds, A.M. and Frye, M.A. (2007) 'Free-flight odor tracking in Drosophila is consistent with an optimal intermittent scale-free search', *PloS One*, Vol. 2, No. 4, p.e354.

Safari, A. and Mekhilef, S. (2010) 'Simulation and hardware implementation of incremental conductance MPPT with direct control method using cuk converter', *IEEE Transactions on Industrial Electronics*, Vol. 58, No. 4, pp.1154–1161.

Saidi, K., Maamoun, M. and Bounekhla, M.H. (2019) 'A new high performance variable step size perturb-and-observe MPPT algorithm for photovoltaic system', *International Journal of Power Electronics and Drive Systems*, Vol. 10, No. 3, p.1662.

Sera, D., Mathe, L., Kerekes, T., Spataru, S.V. and Teodorescu, R. (2013) 'On the perturb-and-observe and incremental conductance MPPT methods for PV systems', *IEEE Journal of Photovoltaics*, Vol. 3, No. 3, pp.1070–1078.

Sher, H.A., Murtaza, A.F., Noman, A., Addoweesh, K.E., Al-Haddad, K. and Chiaberge, M. (2015) 'A new sensorless hybrid MPPT algorithm based on fractional short-circuit current measurement and P&O MPPT', *IEEE Transactions on Sustainable Energy*, Vol. 6, No. 4, pp.1426–1434.

Shivakumar, R., Lakshmipathi, R. and Chandrasekaran, M. (2012) 'Multimachine stability analysis using meta-heuristic PSO algorithm for HGTG and SGTG systems', *International Journal of Modelling, Identification and Control*, Vol. 15, No. 1, pp.55–68.

Singh, N.A., Muraleedharan, K.A. and Gomathy, K. (2009) 'An intelligent neuro-fuzzy logic controller for induction generator based wind generation to improve power system stability', *International Journal of Modelling, Identification and Control*, Vol. 6, No. 3, pp.188–195.

Soufyane Benyoucef, A., Chouder, A., Kara, K. and Silvestre, S. (2015) 'Artificial bee colony based algorithm for maximum power point tracking (MPPT) for PV systems operating under partial shaded conditions', *Applied Soft Computing*, Vol. 32, pp.38–48.

Sun, X. and Zhu, H. (2012) 'Artificial neural networks inverse control of 5 degrees of freedom bearingless induction motor', *International Journal of Modelling, Identification and Control*, Vol. 15, No. 3, pp.156–163.

Tajuddin, M.F.N., Ayob, S.M., Salam, Z. and Saad, M.S. (2013) 'Evolutionary based maximum power point tracking technique using differential evolution algorithm', *Energy and Buildings*, Vol. 67, pp.245–252.

Titri, S., Larbes, C., Toumi, K.Y. and Benatchba, K. (2017) 'A new MPPT controller based on the ant colony optimization algorithm for photovoltaic systems under partial shading conditions', *Applied Soft Computing*, Vol. 58, pp.465–479.

Tudorache, T. and Kreindler, L. (2010) 'Design of a solar tracker system for PV power plants', *Acta Polytechnica Hungarica*, Vol. 7, No. 1, pp.23–39.

Wang, S. (2021) 'Asymptotic tracking control for nonaffine systems with disturbances', *IEEE Transactions on Circuits and Systems II: Express Briefs*, Vol. 69, No. 2, pp.479–483.

Wang, S., Na, J. and Chen, Q. (2020) 'Adaptive predefined performance sliding mode control of motor driving systems with disturbances', *IEEE Transactions on Energy Conversion*, Vol 36, No. 3, pp.1931–1939.

Yang, X.S. and Deb, S. (2009) 'Cuckoo search via Lévy flights', in *2009 World Congress on Nature & Biologically Inspired Computing (NaBIC)*, IEEE, December, pp.210–214.

Yang, Y. and Zhao, Q. (2012) 'Machine vibration prediction using ANFIS and wavelet packet decomposition', *International Journal of Modelling, Identification and Control*, Vol. 15, No. 3, pp.219–226.

Zou, Y., Yan, F., Wang, X. and Zhang, J. (2020) 'An efficient fuzzy logic control algorithm for photovoltaic maximum power point tracking under partial shading condition', *Journal of the Franklin Institute*, Vol. 357, No. 6, pp.3135–3149.